UNIVERSITY OF BIRMINGHAM
University of Birmingham Research at Birmingham

Characteristics and large-scale drivers of atmospheric rivers associated with extreme floods in New Zealand

Kingston, Daniel G.; Lavers, David A.; Hannah, David M.

DOI:
10.1002/joc.7415

License:
None: All rights reserved

Document Version
Peer reviewed version

Citation for published version (Harvard):
Kingston, DG, Lavers, DA & Hannah, DM 2021, 'Characteristics and large-scale drivers of atmospheric rivers associated with extreme floods in New Zealand', *International Journal of Climatology*.
https://doi.org/10.1002/joc.7415

Link to publication on Research at Birmingham portal

Publisher Rights Statement:
his is the peer reviewed version of the following article: Kingston, D. G., Lavers, D. A., & Hannah, D. M. (2021). Characteristics and large-scale drivers of atmospheric rivers associated with extreme floods in New Zealand. International Journal of Climatology, which has been published in final form at https://doi.org/10.1002/joc.7415. This article may be used for non-commercial purposes in accordance with Wiley Terms and Conditions for Use of Self-Archived Versions. This article may not be enhanced, enriched or otherwise transformed into a derivative work, without express permission from Wiley or by statutory rights under applicable legislation. Copyright notices must not be removed, obscured or modified. The article must be linked to Wiley's version of record on Wiley Online Library and any embedding, framing or otherwise making available the article or pages thereof by third parties from platforms, services and websites other than Wiley Online Library must be prohibited.

General rights
Unless a licence is specified above, all rights (including copyright and moral rights) in this document are retained by the authors and/or the copyright holders. The express permission of the copyright holder must be obtained for any use of this material other than for purposes permitted by law.

•Users may freely distribute the URL that is used to identify this publication.
•Users may download and/or print one copy of the publication from the University of Birmingham research portal for the purpose of private study or non-commercial research.
•User may use extracts from the document in line with the concept of 'fair dealing' under the Copyright, Designs and Patents Act 1988 (?)
•Users may not further distribute the material nor use it for the purposes of commercial gain.

Where a licence is displayed above, please note the terms and conditions of the licence govern your use of this document.

When citing, please reference the published version.

Take down policy
While the University of Birmingham exercises care and attention in making items available there are rare occasions when an item has been uploaded in error or has been deemed to be commercially or otherwise sensitive.

If you believe that this is the case for this document, please contact UBIRA@lists.bham.ac.uk providing details and we will remove access to the work immediately and investigate.

Download date: 09. Apr. 2024

Characteristics and large-scale drivers of atmospheric rivers associated with extreme floods in New Zealand

Short title: Atmospheric rivers and floods in New Zealand

Kingston, D. G.[1]*, Lavers, D. A.[2,3] and Hannah, D. M.[3]

[1] School of Geography, University of Otago, Dunedin, New Zealand

[2] European Centre for Medium-Range Weather Forecasts, Reading, UK

[3] School of Geography, Earth and Environmental Sciences, University of Birmingham, Birmingham, UK

*corresponding author

email daniel.kingston@otago.ac.nz

phone +64 21 4798971

Co-author emails: David.Lavers@ecmwf.int; D.M.HANNAH@bham.ac.uk

Re-submitted to the International Journal of Climatology

September 2021

See acknowledgements for details of data availability.

Abstract

The Southern Alps in the South Island of New Zealand are one of wettest places globally, making it critical to understand the mechanisms for delivery of extreme precipitation and river flooding. Atmospheric rivers (ARs) are recognised as key causes of extreme precipitation in New Zealand, but relatively little is known about their large-scale meteorological drivers. Here, we aim to investigate these hydroclimatological connections for five major South Island catchments located from south-north along the axis of the Southern Alps: Te Anau, Matukituki, Pūkaki, Rakaia and Waiau Toa. For each catchment, the top eight flood events over a 38-year period are characterised. Specifically, vertically integrated horizontal water vapour transport (IVT), 500 hPa geopotential and 300 hPa winds are examined to quantify the large-scale atmospheric drivers of flood events. The Kidson synoptic weather classification is also employed to understand better the connection of IVT to New Zealand weather patterns. Intense IVT is associated with flood events for all five catchments and, in most instances, corresponds to AR-type events. Spatial patterns of IVT display substantial variation between flood events and catchments; however, there are some generalizable patterns. Firstly, clear AR-type IVT patterns dominate for all catchments (except the Waiau Toa) with AR orientation ranging from westerly to northwesterly. For the most northerly catchment (Waiau Toa), cyclonic zones of high IVT occur instead for some events. Secondly, AR length varies from those restricted to the Tasman Sea (~ 2000 km) to those extending to the west or north of Australia. Thirdly, northwesterly ARs are associated with the passage of a depression in the general westerly circulation, characterised in particular by the Kidson 'Trough' weather type. Finally, AR orientation is associated strongly with 300 hPa winds, and in many cases to the general wave characteristics of Southern Hemisphere circulation, particularly the Zonal Wave 3 pattern.

Key words: Atmospheric rivers, floods, atmospheric water vapour flux, New Zealand

Introduction

Extremely high rainfall along the main divide of the Southern Alps/Kā Tiritiri o te Moana in New Zealand makes this region one of the wettest places globally, and so a location where mechanisms for delivery of extreme precipitation totals are critical to understand. These high precipitation amounts mean that the Southern Alps act as 'water towers' for the much drier areas to the east (Vivroli et al. 2007), where water from the rivers originating in the Southern Alps is used intensively for electricity generation and irrigated agriculture. Just as this multi-scale perspective is needed to understand terrestrial hydrology, precipitation delivery is also influenced by a number of interacting climate variables across different scales (Kingston et al. 2020). For New Zealand, these include weather systems of tropical, temperate and sub-polar origin, themselves affected by hemispheric-scale atmospheric circulation patterns such as the Southern Annular Mode (SAM; Kidston et al. 2009) and El Nino Southern Oscillation (ENSO; Gordon 1986). Irrespective of their origin, these weather systems are all subject to strong topographic modification across New Zealand's mountain terrain.

A handful of global-scale studies have identified New Zealand as being strongly affected by landfalling atmospheric rivers (ARs), which are synoptic features responsible for transporting the majority of water vapour in the warm sector of mid-latitude cyclones. Strikingly, global-scale analyses have shown that up to 80% of annual river flow can be associated with ARs in some parts of the country (Paltan et al. 2017). These impacts may be exacerbated in the future as New Zealand is a hotspot for projected climate change impacts on ARs (Espinoza et al. 2018), with ARs in general expected to increase in their magnitude and duration (Douville et al. 2021). Studies focussed directly on New Zealand have provided further support for the importance of ARs. Similar to the findings of Paltan et al. (2017), Prince et al. (2021) showed that over 70% of total precipitation in locations on the west coast of the South Island/Te Waipounamu occurred during or within 12 hours of AR arrival, and an even higher proportion of extreme (98^{th} percentile) precipitation (>80%). Although their importance diminishes away from the west coast and topographic forcing associated with the Southern Alps, ARs were shown to remain critical to precipitation climatology across a series of locations around New Zealand. In subsequent studies, both Reid et al. (2021) and Shu et al. (2021) have found a similarly dominant role of ARs for extreme precipitation events across New Zealand. Furthermore, these broad characteristics of New Zealand AR climatology are reflected in more geographically focussed studies within New Zealand, and from precipitation to river flows and the cryosphere. For example, ARs have been shown to be critical for extreme high flow events in the headwaters of the Waitaki river (Pūkaki catchment) that drains eastwards from the Southern Alps

(Kingston et al. 2016), as well as for major snowfall and ablation events at study sites within the Southern Alps (Cullen et al. 2019; Little et al. 2019; Porhemmat et al. 2020; Porhemmat et al. 2021). As with other locations around the world that commonly experience ARs, in New Zealand their impact ranges from beneficial for more moderate events (i.e. providing water for irrigation and hydroelectric storage schemes), to damaging for the most extreme events (Prince et al. 2021). Floods are the most common cause of high-magnitude insurance losses from natural disasters in New Zealand (McAneney et al. 2021).

Although these previous studies have firmly established the importance of ARs for the hydroclimatology of New Zealand, many unanswered questions remain regarding the nature of the weather systems that lead to AR occurrence, and in turn the relationship to driving features of the regional and larger scale climate system such as SAM and ENSO. Moreover, little is known about how the importance of these climate system features vary for ARs occurring over different parts of NZ – this is important, given its topographical complexity and the extreme climatic gradients that result (e.g. Sturman et al. 1999). Bearing in mind these research gaps, the following questions are addressed in this study: 1) how does the AR influence on floods vary spatially across the South Island/Te Waipounamu; 2) how does AR magnitude and structure vary between events and locations; and 3) what are the links between ARs across the South Island and large-scale climate patterns. By answering these questions, we aim to enhance understanding of the hydroclimatological process cascade connecting to regional climate, ARs and extreme floods in New Zealand.

Data and Methods

The top eight river flow events from 1979-2018 are investigated for tributaries or upper reaches of five major catchments across the South Island of New Zealand (Figure 1). These study catchments include some of the major hydroelectricity power stations in New Zealand, alongside providing water for large irrigation schemes and important, biodiverse habitats. From south to north, the Lake Te Anau inflow record (3100 km^2) is used as representative of the larger Waiau catchment (8314 km^2; part of the 850 MW Manapouri hydropower scheme. The Matukituki at West Wānaka (800 km^2) is a headwater tributary of the Clutha/Mata Au, New Zealand's largest catchment (20,582 km^2). The Clutha includes two major hydroelectric power stations (Roxburgh and Clyde), comprising 784 MW generating capacity in total. The Lake Pūkaki catchment (1457 km^2) forms one of the three headwater lake catchments for the Waitaki (11,900 km^2), draining eastwards from the central zone of the Southern Alps. The Waitaki was also the study focus of Kingston et al. (2016), and is the most

important catchment for hydro-electricity generation nationally (1738 MW generating capacity across seven power stations). The Rakaia catchment is gauged at Fighting Hill (2560 km^2), covering the montane runoff generating area that comprises the majority of this catchment (2800 km^2). There is a relatively small hydroelectric scheme on this river (34 MW). Below the gauging station the Rakaia broadens into a large braided river, and also services the largest irrigation scheme in the South Island (the Central Plains Water Enhancement Scheme). Finally, the 3154 km^2 Waiau Toa/Clarence is represented by the Jollies station record (440 km^2). In contrast to the other catchments, the Waiau Toa largely flows through wilderness areas, with comparatively little direct abstraction or modification of river flow. Lake inflow data were provided by Meridian Energy for Lakes Te Anau and Pūkaki; the National Institute for Water and Atmospheric Research (NIWA) provided data for the other three study catchments.

The top eight absolute highest flow events were identified from mean daily discharge records from each river/lake catchment. Events were required to be independent – defined by river flow returning to (approximate) monthly average values between events and a minimum seven-day separation between events. Although river flow in all study catchments is modified to some extent by human activity, either this predominantly influences low rather than high flows, occurs primarily in a downstream location, or a naturalised record is used. Specifically, for the Matukituki the river flow record at West Wānaka (near the river outlet to Lake Wānaka) is not substantially modified. The upstream locations of the discharge records used for the Rakaia and Waiau Toa were chosen due to the occurrence of abstractions (primarily for irrigation) in the lower sections of these catchments. Similarly, inflow data for Lakes Pūkaki and Te Anau are naturalised records for two catchments (the Waitaki and Waiau) that are managed intensively for hydropower at the lake outlet and for irrigation purposes further downstream. Correspondingly, hydroclimatological connections for extreme high flows can be explored largely independently of human influence on the land surface.

The Matukituki, Pūkaki and Rakaia catchments have their lowest seasonal flows in the austral winter, with peaks in spring or summer (Figure 2). This seasonal cycle corresponds closely to the storage and melt of seasonal snow, as the snow line moves from approximately 1000 to 2500 m between winter and summer (Fitzharris et al. 1999). The Matukituki, Pūkaki and Rakaia are partly fed by glacial meltwater, although snow storage and melt are proportionally far more important (e.g. Jobst et al. 2018; Kerr 2013). The headwaters of these three catchments are located in the highest parts of the Southern Alps (with the highest peak, Aoraki/Mount Cook at 3724 m), again indicating the dominant role of snow storage and release for the annual river flow regime. This is also reflected in the highest extreme flow events occurring primarily during spring and summer. The more

145 southerly Lake Te Anau catchment has a somewhat smaller snow influence, with the seasonal regime
146 (and occurrence of extreme events) less pronounced, but still peaking in spring and summer (Figure
147 2). In addition to mid-winter low flows, the annual minimum for Lake Te Anau is actually
148 experienced in February, again reflecting the earlier cessation of snowmelt input compared to the
149 middle three catchments. In contrast to the lower four catchments, the Waiau Toa rises in the inland
150 Kaikōura range, a northeastern extension of the Southern Alps. The inland Kaikōura range is both
151 further from the west coast and lower in altitude than other catchments (highest elevation 2885 m, at
152 Tapuae-o-Uenuku). Although the annual regime of the Waiau Toa peaks in spring (again, associated
153 with snowmelt), it maintains relatively high river flow through winter, with the annual minimum
154 occurring during February (Figure 2). High flow extremes are distributed relatively evenly from
155 winter through to late spring.

156 The widely used Kidson synoptic weather classification (Kidson 2000) is applied here to characterise
157 the meteorological situation associated with high flow events for the five study catchments. The
158 Kidson scheme is based on a combination of principal components analysis and cluster analysis of
159 1000 hPa geopotential data from the NCEP/NCAR reanalysis (Kalnay et al. 1996), with synoptic
160 types assigned twice daily, at 00 and 12 UTC. There are 12 individual synoptic types, which can be
161 grouped into three broad regimes: trough, westerly and blocking (Kidson 2000). These regimes are
162 associated with distinct patterns of temperature and precipitation across New Zealand (Renwick
163 2011).

164 To identify the meteorological situation associated with the occurrence of extreme high river flows at
165 each study site, and in particular the role of ARs, vertically integrated horizontal water vapour
166 transport (IVT) was analysed for each instance. This was performed, at 6-hour time-steps, using the
167 ERA5 reanalysis data set (Hersbach et al. 2020): specifically the northwards and eastwards IVT
168 fields, IVT divergence field, as well as 500 hPa geopotential and 300 hPa U- and V-components of
169 wind. Bearing in mind the event-based focus of this study, the presence of ARs were not formally
170 tested using an auto-detection algorithm such as that presented by Guan and Waliser (2015). Instead,
171 IVT magnitude (> 250 kg m^{-1} s^{-1}), spatial pattern of IVT (i.e. length/width ratio >2) and connection
172 to a low pressure system were used to manually identify IVT patterns as corresponding to ARs,
173 following the general definition of ARs provided by Ralph et al. (2017).

174

175 **Results and Discussion**

176 *Flood timing and magnitude*

Flood events for the four southernmost catchments (Te Anau, Matukituki, Pūkaki and Rakaia) occur primarily during the austral summer half year (27 of 36 events), and in particular the peak summer months of December and January (19 events; Figure 2). This concentration is particularly the case for Pūkaki and Rakaia, which between them have just two events outside the November-January period (March for Pūkaki, and May for Rakaia). The highest flood events also typically occur in December-January for these four catchments. The timing of Te Anau flood events is just slightly more variable than the other three, with two floods also recorded in the mid-winter months of August and June (the 5th and 7th ranked events, respectively).

The concentration of flood events during summer months for the four southernmost catchments strongly indicates the augmentation of extreme rainfall totals by seasonal snowmelt for flood events, with all having their headwaters at elevations above the seasonal snowline in the Southern Alps. Furthermore, the catchment with the strongest concentration of flood events in peak summer, Pūkaki, also has the highest elevation headwaters and highest contribution of snowmelt to river flow (23%; Kerr, 2013).

In contrast to the other four catchments, Waiau Toa floods are relatively evenly spread through the year (Figure 2), although with some grouping of events during the winter-early spring period (four from July to September). This difference from the other four catchments reflects the location of the Waiau Toa headwaters in the Inland Kaikōura range, which is both at a lower elevation and located further east (and so drier) than the more central region of the Southern Alps where the other study catchments are located. The resultant higher rain: snow ratio and lower overall precipitation totals for the Waiau Toa lead to the greater occurrence of flood events year-round, and slight tendency of rain-on-snow flood peaks to occur more commonly in winter, rather than spring and summer.

Alongside similarities in seasonality, there are some common flood event timings between catchments, particularly for the two more central catchments: Pūkaki (four out of eight events are coincident with top eight floods in other catchments) and Rakaia (six coincident events). However, there are no common events between the furthest north and south catchments (Waiau Toa and Te Anau, respectively).

Differences in flood magnitude across the five catchments corresponds broadly to differences in catchment size – i.e. the highest magnitude floods occur for Te Anau (up to 4656 $m^{-3}\,s^{-1}$), and lowest for Waiau Toa (maximum of 263 $m^{-3}\,s^{-1}$). However, for the four southernmost catchments the proportional departure from monthly average flow is relatively consistent. Once discharges have been standardised relative to their respective monthly mean and standard deviation, the monthly z-

score values for the flood discharge range between approximately 6 and 14. In contrast, flood magnitudes for the smaller Waiau Toa are proportionally higher, with z-scores ranging from 12-22. This may indicate that where ARs intersect with smaller catchments there is a greater likelihood of extreme discharge, given that more of the catchment is exposed to the AR.

IVT and local circulation characteristics during flood events

All flood events for all five study locations occur in conjunction with IVT immediately upwind of the catchment above the nominal 250 kg m^{-1} s^{-1} threshold for AR occurrence (Gimeno et al. 2014; Figures 3-7). Higher IVT values are typically present upwind of the study catchments, with a maximum IVT of over 1800 kg m^{-1} s^{-1} for Pūkaki event 6/Rakaia event 3. With flux magnitudes >1250 kg m^{-1} s^{-1} in many instances across all five catchments, a number of systems fall into the maximum AR intensity category proposed by Ralph et al. (2019) – although these values drop substantially as the system reaches the catchment gauge/outlet (Table 1). Overall, the strongest IVT systems occur for Te Anau, Pūkaki and Rakaia floods, with the Waiau Toa systems generally the weakest.

Although an important precursor to floods, high IVT values in themselves are not a direct indicator of extreme precipitation and river flow. Substantial moisture convergence is necessary for the most extreme precipitation events in the Southern Alps (Sinclair et al. 1997, Chater and Sturman 1998). Correspondingly, ouranalysis reveals strong areas of IVT convergence immediately upwind of the study catchments associated with the top eight flood events for the lower four catchments (Figures S1-S4), and most of the Waiau Toa events (Figure S5). Furthermore, IVT direction is close to perpendicular to the approximate northeast-southwest orientation of the Southern Alps across all events for the Te Anau, Matukituki, Pūkaki and Rakaia catchments (Table 1). For Waiau Toa, similar perpendicular IVT – topography orientations are found, but with some events from the northwest and others from the opposite southeast direction. As such, these results indicate clearly that weather systems with high IVT and subsequent convergence associated with orographic forcing as the primary cause of the precipitation that drives these extreme flood events. Snowmelt is likely to be a contributing factor during the period from winter to early summer, bearing in mind the tendency for AR-bearing weather systems to be associated with warmer air (e.g. Little et al. 2019).

The spatial form of the areas of high IVT for most events for the four southernmost catchments are broadly consistent with ARs, consisting of long and relatively thin zones of IVT>250 kg m^{-1} s^{-1} (Figures 3-6). A smaller number of events have much wider zones of high IVT. In some cases these

241 are wide and long zones of high IVT, associated with less distinct or possibly closely following
242 weather systems (e.g. Matukituki events 3 and 4; Figure 4). For five Waiau Toa flood events (1-3, 5,
243 7), there are strongly circular high IVT patterns that are centred to the north of New Zealand (Figure
244 7). In contrast to the Tasman and Southern Ocean systems that dominate for the four southernmost
245 catchments, these Waiau Toa systems are more difficult to describe in terms of typical length: width
246 ratios due to their circular nature.

247 The weather systems that lead to high IVT and flood events for the four southern catchments consist
248 generally of an eastward-propagating low pressure trough passing over or to the south of New
249 Zealand, leading to a northwesterly AR orientation at landfall. Many of these high IVT systems are
250 part of a series of depressions embedded in the mid-latitude westerlies, with each depression
251 containing a northwesterly orientated AR (e.g. Te Anau events 1 and 3, Pūkaki event 6/Rakaia event
252 3: Figures 3, 5 and 6). These systems extend across the majority of the width of the Tasman Sea
253 towards the east coast of Australia, and in some cases a substantial distance into the continent (e.g.
254 Matukituki event 2 vs. Te Anau event 1: Figures 4 and 3). Irrespective of how far these
255 northwesterly systems extend into the Australian continent, they are associated commonly with the
256 troughing regime of the Kidson synoptic classification for New Zealand (Kidson 2000), indicating
257 the passage of a low pressure trough over New Zealand (Figure 8). When totalled across all events
258 for all catchments, the troughing regime occurs for 57% of the time during the rising limb of flood
259 hydrographs (Figure 9). The Trough weather type within the Kidson troughing regime is particularly
260 common, occurring during 35% of the time and comprising the most common type for Pūkaki and
261 Rakaia flood events, and second most common type for the other three study catchments. The
262 Trough type is associated with strong NW-W-SW airflow from the west to east of the South Island
263 (respectively) and a low pressure system centred in the Southern Ocean (Figure 8), and so matches
264 well the geopotential height and IVT fields associated with many high flow events (Figures 3-7). The
265 Trough type has previously been shown to be associated with increased precipitation across much of
266 New Zealand (Renwick 2011) and ARs in the Pūkaki catchment (Kingston et al. 2016). Other
267 weather types associated with northwesterly airflow and the passage of a trough over the South
268 Island coincide commonly with AR events too: TNW (troughing regime, 15% of the time) and HE
269 (blocking regime, 19%).

270 Notwithstanding the strong connection between the majority of extreme river flow events and the
271 Trough weather type for the southern four catchments, a smaller number of events are instead linked
272 to relatively isolated cyclonic weather systems that are part of a more strongly westerly circulation
273 regime (e.g. Te Anau event 2/Rakaia event 4, Te Anau event 5; Figures 3 and 6). These typically

contain relatively long zones of high IVT, continuing uninterrupted across the Southern Ocean and past the western limits of Australia. Correspondingly, these events are more commonly associated with the Westerly type (Zonal regime; Figure 8), occurring over 13% of the time during the flood hydrograph rising limb, but the most common type for Te Anau. The Zonal regime has been linked to increased precipitation in the southwest of the South Island before (Renwick 2011) but not yet to ARs.

In contrast to the westerly quadrant origin of high IVT and AR-producing weather systems that predominate for the four southern catchment events, the five Waiau Toa events originating from circular IVT patterns are instead associated with easterly moisture flux over the catchment. Although these are still associated with depressions moving in a broadly westerly direction, these are centred to the north of New Zealand rather than the south (Figure 7), meaning that the Waiau Toa experiences the easterly flow associated with the southernmost section of the (clockwise rotating) cyclonic system. As the Waiau Toa is located some way east of the Main Divide of the Southern Alps in comparison to the other catchments, these strong easterly moisture fluxes (and associated IVT divergence) can yield substantial precipitation. For these E-NE systems, the TSW and R Kidson weather types are most commonly observed, which have a low pressure centred over or to the north of New Zealand and relatively widely spaced isobars (Figure 8), consistent with the geopotential height and IVT patterns for these events.

Large-scale meteorological drivers of AR and flood events

Despite the importance of the mid-latitude westerlies for the occurrence of AR-producing weather systems, flood events do not occur consistently across either strong positive, negative or neutral Southern Annular Mode (SAM) situations: the average daily SAM index value across the top eight events for each catchment is within the -1 to +1 range, and each catchment has flood events that occur for index values above +1 and below -1 (Table 2). There is little evidence of consistent differences either between AR strength, orientation and extent with the SAM. For example, Waiau Toa events 1 and 2 are both associated with easterly IVT and a cyclonic weather system centred over the North Island, yet the event 1 SAM index is +1.17 whereas for event 2 it is -0.94. Similarly, relatively similar high IVT/AR events associated with Southern Ocean depressions and northwesterly flow over the South Island can also occur under substantially different SAM index values: e.g. -1.83 for Te Anau event 1 vs. 1.31 for Te Anau event 7 (Figure 3). Although in each case the poleward/equatorward movement of the mid-latitude westerlies can be seen between positive and

negative SAM index situations, apparently similar flood-producing weather events are still observed from a New Zealand perspective. This situation perhaps reflects the difficulty of describing relatively local-scale conditions using a large-scale circulation index (Kingston et al. 2006; Lavers et al. 2010).

Irrespective of the connection to the SAM and the strength and latitude of the mid-latitude westerlies, there is strong association between the presence of high IVT values and the concurrent location of strong upper atmosphere winds (i.e. the jet stream) in the New Zealand-Tasman Sea region during each flood event (Figure 8, and Figures S6-10). Ralph et al. (2004) and Cordeira et al. (2013) have previously developed conceptual models of the connection between ARs and jet stream patterns based on findings from the North Pacific (see also Ralph et al. 2017). In terms of the larger-scale context for upper atmosphere winds and New Zealand climate, two jet stream configurations dominate: either the presence of both the subtropical and polar front jets (i.e. a split-jet situation), or a just a single jet stream in the New Zealand region (Gallego et al. 2005). Previous studies have focussed primarily on the relationship of jet stream configuration to the mass balance of glaciers Southern Alps (Clare et al. 2002; Cullen et al. 2019; Mackintosh et al. 2017; Tyson et al. 1997), but more recently Prince et al. (2021) explored the connection to the AR climatology of New Zealand. In particular, the climatological position of the polar jet at 50 °S during the austral summer half year was shown to be important for ARs on the South Island west coast, with a split jet situation more conducive to ARs on the east coast.

Here, distinct configurations for the two jets are shown across extreme IVT patterns (including ARs) associated with floods for the different catchments in both summer and winter – with variation in IVT patterns between events and catchments mirrored by differences in 300 hPa winds. As exemplified in Figure 10 (and shown on an event-by-event basis in Figures S6-S10), the cyclonic systems leading to northeasterly IVT and high river flows in the Waiau Toa are associated with a clear separation of the subtropical and polar jets – following the findings of Prince et al. (2021). Reflecting their origin in the Southern Ocean (rather than the sub-tropics), zonally extensive events as exemplified by Rakaia event 4 (Figure 6) are linked to a single and much stronger jet stream located between 40-55 °S (Figure 10). Other events fall somewhere in between these two general typologies, for both summer and winter season high flow events: for example, ostensibly separate jets but with some overlap associated with individual weather systems (e.g. Te Anau event 7); or a predominantly Southern Ocean polar jet system with residual connection to lower latitudes (e.g. Matukituki event 2). Irrespective of the jet configuration, peak IVT during flood events is typically spatially coincident with strong upper atmosphere winds and in particular a strong north-to-south directional component (i.e. the preceding limb of the trough). Hence, these results further highlight

the key connection between ARs, extratropical cyclones and the jet stream configuration in the New Zealand sector.

Consistent with the apparent relationship between circulation troughs at both the surface (i.e. Kidson weather types) and in the upper atmosphere, there is also some connection to the presence of zonal waves in the general Southern Hemisphere circulation. Although Southern Hemisphere extratropical circulation is largely zonally symmetric, some zonal asymmetry is superimposed (e.g. Fogt et al. 2012; Irving and Simmonds 2015; Raphael 2004). These zonal wave patterns are quasi-stationary and are dominated by a zonal wave 1 and 3 pattern (ZW1 and ZW3). As such, indices of annular circulation characteristics (i.e. the SAM) can be insufficient as the sole descriptor of southern hemisphere circulation. For example, Garreaud et al. (2013) found that zonal asymmetry was more important for variation in Patagonian precipitation compared to the annular mode (Patagonia is the approximate location of one of the ZW3 ridges). Similarly, ZW3 is of particular interest in the context of New Zealand weather given that another of the three quasi stationary ridges is located at approximately 166 °E (Raphael 2004), i.e. within the New Zealand domain. Furthermore, teleconnections have been described between New Zealand glacier mass balance and dry spells in South Africa (Tyson et al. 1997), close to the approximate location of the third ZW3 ridge.

An index of ZW3 pattern strength can be calculated by averaging the standardised zonal 500 hPa geopotential height anomaly at the location of the three quasi-stationary ridges of the wave (Raphael 2004). Here, a daily ZW3 index based on ERA-Interim 500 hPa geopotential height data was used (Raphael 2004). Positive ZW3 values indicate strong wave activity across the Southern Hemisphere, and thus a stronger meridional component, and *vice versa* (Figure S11). Although AR-driven flood events occur during both positive and negative phases of the ZW3 index, the mean daily ZW3 index value across the top eight flow events for all five rivers is negative: from -0.16 (Pūkaki) to -0.43 (Matukituki) (Table 3). Out of the 40 events analysed across all rivers, only nine occur under positive ZW3 conditions, with only one of these more than one standard deviation away from the longer term mean of zero (Pūkaki event 7). In contrast, 18 events have negative ZW3 values more than one standard deviation away from the mean (i.e. index value of +/- 0.5). Thirteen of these events are coincident with a Kidson Trough weather type. The strongest individual negative value is -1 (Te Anau event 4), with a highest positive value of 0.6 (Pūkaki event 7). As such, the results suggest some predisposition to ARs and flood events occurring in a negative ZW3 situation. This relationship becomes even more apparent from comparison of the ZW3-geopotential height correlation (Figure S11) and geopotential patterns associated with ARs and extreme flood events (Figures 3-7). Specifically, ZW3 is positively correlated with geopotential height to the south and

southwest of New Zealand, whereas ARs and associated flood events occur frequently in association with an area of low pressure to the southwest of New Zealand.

Alongside connections to the zonality of the Southern Hemisphere mid-latitude circulation, links to tropical latitudes are evident for some flood events. In some cases these are located over the western Pacific/coastal Queensland region (e.g. Pūkaki event 6). For other events, the zone of high IVT extends into the tropics via the interior of the Australian landmass. In particular, a number of events appear to trace back to (or close to) the Indian Ocean coastline of northwestern Australia (e.g Te Anau events 1, 6-8). As such, these IVT patterns show some resemblance to the Australian northwest cloudband weather pattern (albeit with a Tasman Sea extension) that has been shown to originate in the Indian Ocean (Tapp and Barrell 1984) and can itself be associated with ARs over Australia (Chen et al. 2020). The upper atmosphere winds during these events also show some evidence of a connection to the Indian Ocean, via a transient overlap between the subtropical and polar jet streams associated with the westerly passage of isolated mid-latitude depressions (e.g. Te Anau event 7; Figures 3 and 10). The northwest cloudband weather pattern has been documented previously as bringing high rainfall events over a broad zone from northwest to southeast Australia (Tapp and Barrell 1984, Telcik and Pattiaratchi 2014). Winter instances of this pattern appear linked to anomalous meridional SST gradients in the Indian Ocean, with the cloud band during summer driven by low pressure anomalies over northwest and central Australia (Reid et al. 2019). Although Mullan (1998) found some connection from Indian Ocean sea surface temperatures to New Zealand precipitation associated with the northwest cloudband pattern, its extension towards and importance of this pattern for New Zealand climate has not been widely studied. However, the apparent correspondence of these high IVT/high river flow events with a northwest cloudband-type pattern suggests this may be a promising direction for further study of large-scale meteorological drivers of New Zealand precipitation – alongside other connections to the tropics via the Madden-Julian Oscillation (Fauchereau et al. 2016).

Conclusions

High magnitude IVT is associated with major flood events across five major catchments along a meridional transect across the South Island of New Zealand. In most instances, IVT fields indicate that these flood events are the result of AR occurrence. In a few cases, IVT patterns reach AR magnitude but do not match the conventional AR spatial pattern. In particular, these IVT patterns

correspond to the most northerly study catchment (the Waiau Toa), which is also located closest to the east coast – and so furthest away from the Main Divide of the Southern Alps.

ARs vary widely in magnitude and structure between flood events and catchments, but with some general themes. AR orientation ranges from westerly to northwesterly for the four southernmost catchments (Te Anau, Matukituki, Pūkaki, Rakaia); length varies from those restricted to the Tasman Sea (~ 2000 km) to those extending to the west or north of Australia. For these four southern catchments all flood events are also associated with northwesterly circulation in the immediate vicinity of New Zealand, which in many situations are connected to the passage of a wave depression in the general westerly circulation (i.e. the Kidson trough regime and Trough weather type). In contrast, more than half of the flood events for the more northerly Waiau Toa are associated with easterly or northeasterly water vapour flux, associated with the cyclonic circulation of a low pressure system passing over or to the north of the country. Owing to the strongly curved zone of high IVT, these systems correspond less clearly with the more typical appearance of an AR as a long and thin filament of poleward high IVT values.

AR orientation is associated strongly with upper atmosphere (i.e. jet stream) winds, with ARs occurring under both single and split-jet configurations in the New Zealand region. Wider connections to Southern Hemisphere atmospheric circulation are evident, most consistently to the general wave characteristics of Southern Hemisphere circulation and the ZW3 pattern. Given the local importance of meridional flow (i.e. troughing) for the majority of AR events, and the coincidence of one of the ZW3 ridges in the New Zealand region, the ZW3 index is most often in a negative phase during the occurrence of extreme flood events in the study catchments. Further work is required to better define this emergent ZW3-AR relationship, the possible role of tropical teleconnections from Australian northwest cloudband weather systems to Tasman Sea ARs for New Zealand flood events, as well as the wider role of ENSO in modulating these systems.

Acknowledgements

Kathy Walter (NIWA) and Jennifer Purdie (Meridian Energy; now University of Otago) provided the river flow and lake inflow data. Marilyn Raphael (University of California – Los Angeles) provided the ZW3 data. James Renwick (Victoria University of Wellington) provided the Kidson Weather Type data. Chris Garden (University of Otago) produced Figure 1. This work was initiated during the lead author's time as a Vanguard Fellow at the University of Birmingham Institute of Advanced

Studies. The authors gratefully acknowledge the constructive comments from two anonymous reviewers.

References

Chater, A.M. and Sturman, A.P. (1998), Atmospheric conditions influencing the spillover of rainfall to lee of the Southern Alps, New Zealand. Int. J. Climatol., 18: 77-92.

Jingjing, C., Huqiang, Z., Chengzhi, Y., Hongzhuan, C., Ruping, M. (2020). Case studies of atmospheric rivers over China and Australia: new insight into their rainfall generation. Journal of Southern Hemisphere Earth Systems Science 70, 17-35.

Clare GR, Fitzharris BB, Chinn TJH, Salinger MJ. 2002. Interannual variation in end-of-summer snowlines of the Southern Alps of New Zealand, and relationships with southern hemisphere atmospheric circulation and sea surface temperature patterns. Int. J. Climatol. 22: 107–120.

Cordeira, J. M., Ralph, F. M., & Moore, B. J. (2013). The Development and Evolution of Two Atmospheric Rivers in Proximity to Western North Pacific Tropical Cyclones in October 2010, Monthly Weather Review, 141(12), 4234-4255.

Cullen, N. J., Gibson, P. B., Mölg, T., Conway, J. P., Sirguey, P., & Kingston, D. G. (2019). The influence of weather systems in controlling mass balance in the Southern Alps of New Zealand. Journal of Geophysical Research: Atmospheres, 124, 4514–4529. https://doi.org/10.1029/2018JD030052

Espinoza, V., Waliser, D. E., Guan, B., Lavers, D. A., & Ralph, F. M. (2018). Global analysis of climate change projection effects on atmospheric rivers. Geophysical Research Letters, 45, 4299–4308.

Fauchereau, N., Pohl, B., & Lorrey, A. (2016). Extratropical Impacts of the Madden–Julian Oscillation over New Zealand from a Weather Regime Perspective. Journal of Climate: 29(6), 2161-2175.

Fitzharris, B. B., Lawson, W., & Owens, I. F. (1999). Research on glaciers and snow in New Zealand. Progress in Physical Geography, 23(4), 469-500.

Fogt, R. L., Jones, J. M., & Renwick, J. (2012). Seasonal Zonal Asymmetries in the Southern Annular Mode and Their Impact on Regional Temperature Anomalies, Journal of Climate, 25(18), 6253-6270.

Garreaud, R., Lopez, P., Minvielle, M., & Rojas, M. (2013). Large-Scale Control on the Patagonian Climate, Journal of Climate, 26(1), 215-230.

Gimeno, L., Nieto, R., Vazquez, M., & Lavers, D. A. (2014). Atmospheric rivers: a mini-review. Frontiers in Earth Science, 2(2). https://doi.org/10.3389/feart.2014.00002

Gordon ND. 1986. The Southern Oscillation and New Zealand weather. Mon. Weather Rev. 114: 371–387.

Guan, B., & Waliser, D. E. (2015). Detection of atmospheric rivers: evaluation and application of an algorithm for global studies. Journal of Geophysical Research: Atmospheres, 120, 514–535. https://doi.org/10.1002/2015JD024257

Hersbach, H, Bell, B, Berrisford, P, et al. The ERA5 global reanalysis. Q J R Meteorol Soc. 2020; 146: 1999– 2049. https://doi.org/10.1002/qj.3803

Irving, D., & Simmonds, I. (2015). A Novel Approach to Diagnosing Southern Hemisphere Planetary Wave Activity and Its Influence on Regional Climate Variability, Journal of Climate, 28(23), 9041-9057.

Kalnay, E., Kanamitsu, M., Kistler, R., Collins, W., Deaven, D., Gandin, L., Iredell, M., Saha, S., White, G., Woollen, J., Zhu, Y., Chelliah, M., Ebisuzaki, W., Higgins, W., Janowiak, J., Mo, K. C., Ropelewski, C., Wang, J., Leetmaa, A., Reynolds, R., Jenne, R., and Joseph, D.: The NMC/NCAR 40-Year Reanalysis Project, B. Am. Meteorol. Soc., 77, 437–471, 1996.

Kerr, T. (2013). The contribution of snowmelt to the rivers of the South Island, New Zealand. Journal of Hydrology (New Zealand), 52(2), 61-82.

Kidson JW. 2000. An analysis of New Zealand synoptic types and their use in defining weather regimes. Int. J. Climatol. 20: 299–316.

Kidston J, Renwick JA, McGregor J. 2009. Hemispheric-scale seasonality of the Southern Annular Mode and impacts on the climate of New Zealand. J. Clim. 22: 4759–4770.

Kingston, D., Lavers, D. and Hannah, D. (2016). Floods in the Southern Alps of New Zealand: the importance of atmospheric rivers. Hydrological Processes, 30 (26), 5063-5070.

Kingston D. G., Lawler D. M., McGregor G. R. 2006. Linkages between atmospheric circulation, climate and streamflow in the northern North Atlantic: research prospects. Prog. Phys. Geogr. 30: 143–174.

Kingston, D. G., Massei, N., Dieppois, B., Hannah, D. M., Hartmann, A., Lavers, D. A., & Vidal, J.-P. (2020). Moving beyond the catchment scale: Value and opportunities in large-scale hydrology to understand our changing world. Hydrological Processes, 34(10), 2292-2298. doi: 10.1002/hyp.13729

Lavers, D., Prudhomme, C., Hannah, D. M. (2010) Large-scale climate, precipitation and British river flows: Identifying hydroclimatological connections and dynamics. Journal of Hydrology, 395, 242-255.

Little, K., Kingston, D. G., Cullen, N. J., & Gibson, P. B. (2019). The role of Atmospheric Rivers for extreme ablation and snowfall events in the Southern Alps of New Zealand. Geophysical Research Letters, 46. https://doi.org/10.1029/2018GL081669

Mackintosh, A. N., Anderson, B. M., Lorrey, A. M., Renwick, J. A., Frei, P., & Dean, S. M. (2017). Regional cooling caused recent New Zealand glacier advances in a period of global warming. Nature Communications, 8, 14202. https://doi.org/10.1038/ncomms14202

Mullan, A.B. (1998), Southern hemisphere sea-surface temperatures and their contemporary and lag association with New Zealand temperature and precipitation. Int. J. Climatol., 18: 817-840.

Paltan, H., Waliser, D., Lim, W. H., Guan, B., Yamazaki, D., Pant, R., & Dadson, S. (2017). Global floods and water availability driven by atmospheric rivers. Geophysical Research Letters, 44, 10,387–10,395. https://doi.org/10.1002/2017GL074882

Porhemmat, R, Purdie, H, Zawar-Reza, P, Zammit, C, Kerr, T. The influence of atmospheric circulation patterns during large snowfall events in New Zealand's Southern Alps. Int J Climatol. 2020; 1– 21. https://doi.org/10.1002/joc.6966

Porhemmat, R., Purdie, H., Zawar-Reza, P., Zammit, C., & Kerr, T. (2021). Moisture Transport during Large Snowfall Events in the New Zealand Southern Alps: The Role of Atmospheric Rivers, Journal of Hydrometeorology, 22(2), 425-444.

Prince, H. D., Cullen, N. J., Gibson, P. B., Conway, J., & Kingston, D. G. (2021) A climatology of atmospheric rivers in New Zealand, Journal of Climate, in press.

518 Ralph, F. M., Dettinger, M., Lavers, D., Gorodetskaya, I. V., Martin, A., Viale, M., et al. (2017).
519 Atmospheric rivers emerge as a global science and applications focus. Bulletin of the American
520 Meteorological Society, 98(9), 1969–1973. https://doi.org/10.1175/BAMS-D-16-0262.1

521 Ralph, F. M., Neiman, P. J., & Wick, G. A. (2004). Satellite and CALJET Aircraft Observations of
522 Atmospheric Rivers over the Eastern North Pacific Ocean during the Winter of 1997/98, Monthly
523 Weather Review, 132(7), 1721-1745.

524 Ralph, F. M., Rutz, J. J., Cordeira, J. M., Dettinger, M., Anderson, M., Reynolds, D., Schick, L. J., &
525 Smallcomb, C. (2019). A Scale to Characterize the Strength and Impacts of Atmospheric Rivers,
526 Bulletin of the American Meteorological Society, 100(2), 269-289.

527 Raphael, M. N. (2004), A zonal wave 3 index for the Southern Hemisphere, Geophys. Res. Lett., 31,
528 L23212, doi:10.1029/2004GL020365

529 Reid, K. J., Rosier, S. M., Harrington, L. J., King, A. D. and Lane, T. P. (2021). Extreme rainfall in
530 New Zealand and its association with atmospheric rivers. Environmental Research Letters: 16,
531 044012.

532 Reid, K. J., Simmonds, I., Vincent, C. L., & King, A. D. (2019). The Australian Northwest
533 Cloudband: Climatology, Mechanisms, and Association with Precipitation, Journal of Climate,
534 32(20), 6665-6684.

535 Renwick JA. 2011. Kidson's synoptic weather types and surface climate variability over New
536 Zealand. Weather and Climate 32: 3–23.

537 Shu, J., Shamseldin, A.Y. & Weller, E. (2021). The impact of atmospheric rivers on rainfall in New
538 Zealand. Sci Rep 11: 5869.

539 Sinclair, M. R., Wratt, D. S., Henderson, R. D., & Gray, W. R. (1997). Factors Affecting the
540 Distribution and Spillover of Precipitation in the Southern Alps of New Zealand—A Case Study.
541 Journal of Applied Meteorology: 36(5), 428-442.

542 Sturman A, A. McGowan H, A. Spronken-Smith R. Mesoscale and local climates in New Zealand.
543 Progress in Physical Geography: Earth and Environment. 1999;23(4):611-635.
544 doi:10.1177/030913339902300407

545 Tapp, R., and S. Barrell, 1984: The North-West Australian cloud band: Climatology, characteristics
546 and factors associated with development. J. Climatol., 4, 411–424,
547 https://doi.org/10.1002/joc.3370040406.

548 Telcik, N., and C. Pattiaratchi, 2014: Influence of northwest cloudbands on southwest Australian
549 rainfall. J. Climatol., 2014, 671394, https://doi.org/10.1155/2014/671394.

550 Tyson, P. D., Sturman, A. P., Fitzharris, B. B., Mason, S. J., & Owens, I. F. (1997). Circulation
551 changes and teleconnections between glacial advances on the west coast of New Zealand and
552 extended spells of drought years in South Africa. International Journal of Climatology, 17, 1499–
553 1512.

554 Viviroli, D., H. H. Du¨rr, B. Messerli, M. Meybeck, and R. Weingartner (2007), Mountains of the
555 world, water towers for humanity: Typology, mapping, and global significance, Water Resour. Res.,
556 43, W07447, doi:10.1029/2006WR005653.

Table 1 IVT direction and magnitude over each catchment during the top eight AR events (N.B. mean values for Waiau Toa have been calculated separately for southeasterly and northwesterly events).

	Te Anau		**Matukituki**		**Pukaki**		**Rakaia**		**Waiau Toa**	
	Dir	Mag	Dir	Mag	Dir	Mag	Dir	Mag	Dir	Mag
1	312	722	351	316	317	566	320	388	163	195
2	320	539	360	289	345	339	329	313	136	136
3	322	502	341	281	309	454	324	650	143	160
4	337	699	340	385	331	363	318	476	324	488
5	315	282	342	128	311	452	317	537	149	213
6	326	815	323	551	320	344	332	473	296	258
7	317	383	314	544	331	406	312	432	148	240
8	329	270	333	412	334	441	330	315	332	265
Mean	**322**	**527**	**338**	**363**	**325**	**421**	**323**	**448**	**148 / 317**	**189 / 337**

561 **Table 2** SAM index values for top eight river flow events for each study catchment (mean SAM
562 value per catchment in final row)

Te Anau	Matukituki	Pūkaki	Rakaia	Waiau Toa
-1.83	1.58	0.27	-1.51	1.17
-1.90	2.71	2.71	-1.58	-0.94
1.70	-1.14	1.72	-0.03	1.23
-1.03	2.19	0.66	-1.81	-1.58
0.08	-0.15	-0.23	0.65	0.31
0.18	0.27	-0.03	2.71	0.51
1.31	0.40	-1.42	-0.23	0.63
1.55	2.00	0.35	-2.02	1.63
0.01	**0.98**	**0.5**	**-0.48**	**0.37**

563

564

565 **Table 3** ZW3 index values for top eight river flow events for each catchment (mean ZW3 value for
566 each catchment given in final row).

Te Anau	**Matukituki**	**Pūkaki**	**Rakaia**	**Waiau Toa**
-0.3	-0.5	-0.8	-0.7	0.1
0.4	-0.3	-0.3	-0.6	-0.3
-0.5	-0.7	-0.4	0.1	-0.3
-1	-0.5	-0.2	0.4	-0.6
-0.2	-0.2	-0.5	-0.8	0.1
0.3	-0.8	0.1	-0.3	-0.4
-0.3	0	0.6	-0.5	0
-0.8	-0.4	0.2	-0.6	-0.5
-0.3	**-0.43**	**-0.16**	**-0.38**	**-0.24**

567

568

Figure captions

Figure 1 Location of the five study catchments and corresponding river gauging stations.

Figure 2 Thirty-day running mean of mean (solid line), maximum and minimum (dotted lines) daily river flow for 1979-2018 for the five study rivers, plus the top eight events for each catchment (circles). Note the different y-axis scales.

Figure 3 IVT (kg m^{-1} s^{-1}, shading) and 500 hPa geopotential height (m, isolines) for the Te Anau top eight flow events.

Figure 4 IVT (kg m^{-1} s^{-1}, shading) and 500 hPa geopotential height (m, isolines) for the Matukituki top eight flow events.

Figure 5 IVT (kg m^{-1} s^{-1}, shading) and 500 hPa geopotential height (m, isolines) for the Pūkaki top eight flow events.

Figure 6 IVT (kg m^{-1} s^{-1}, shading) and 500 hPa geopotential height (m, isolines) for the Rakaia top eight flow events.

Figure 7 IVT (kg m^{-1} s^{-1}, shading) and 500 hPa geopotential height (m, isolines) for the Waiau Toa top eight flow events.

Figure 8 1000 hPa geopotential height composites for the 12 Kidson Weather Types (Kidson 2000)

Figure 9 Occurrence (number of 12-hour timesteps) of different Kidson Weather Types during the ascending limb of top eight flood events for each catchment (TA = Te Anau; MT = Matukituki; PK = Pūkaki; RK; RK = Rakaia; WT = Waiau Toa).

Figure 10 300 hPa wind speed (m s^{-1}, shading) and IVT (kg m^{-1} s^{-1}, isolines) for four exemplar high flow events.

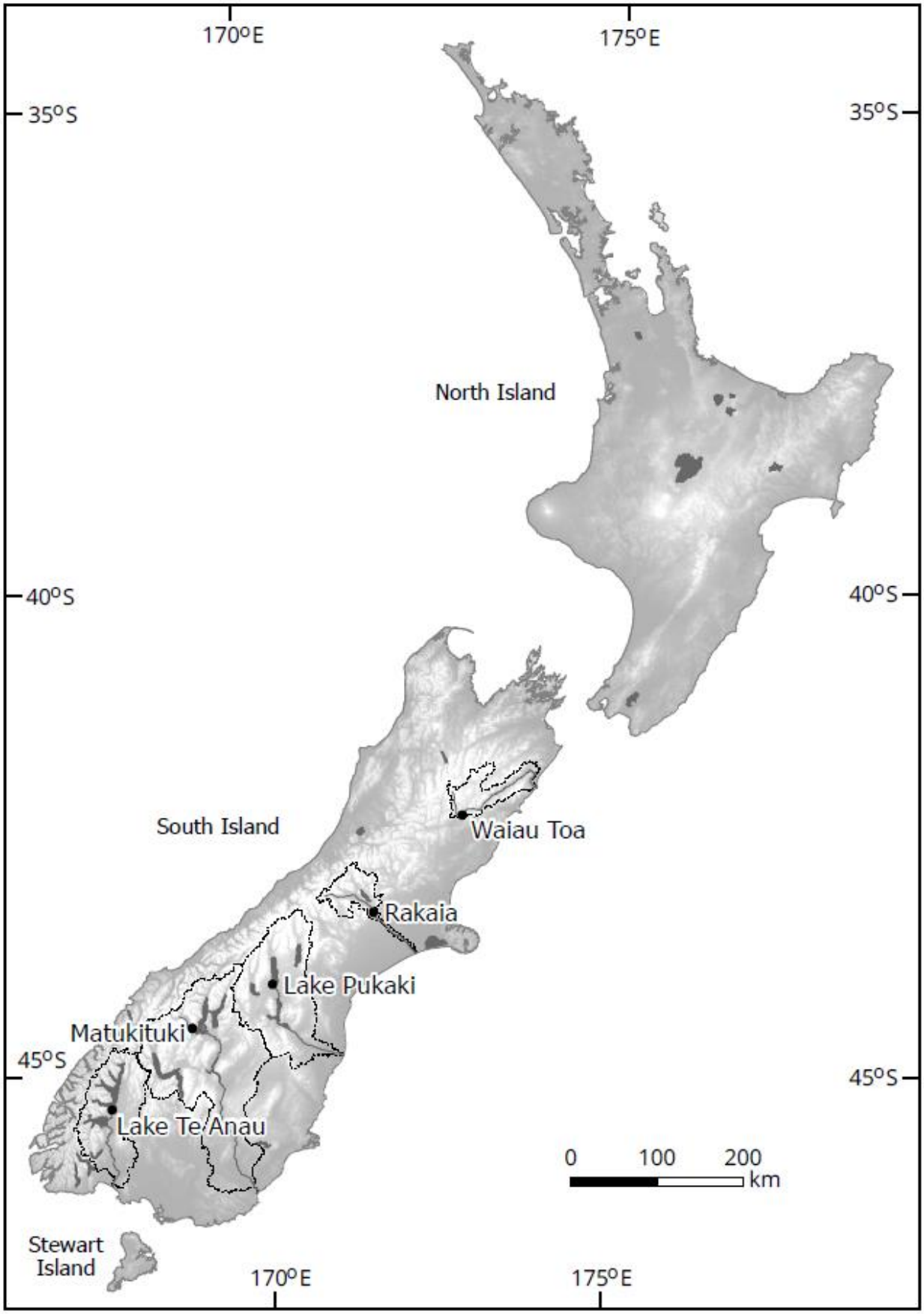

Figure 1 Location of the five study catchments and corresponding river gauging stations.

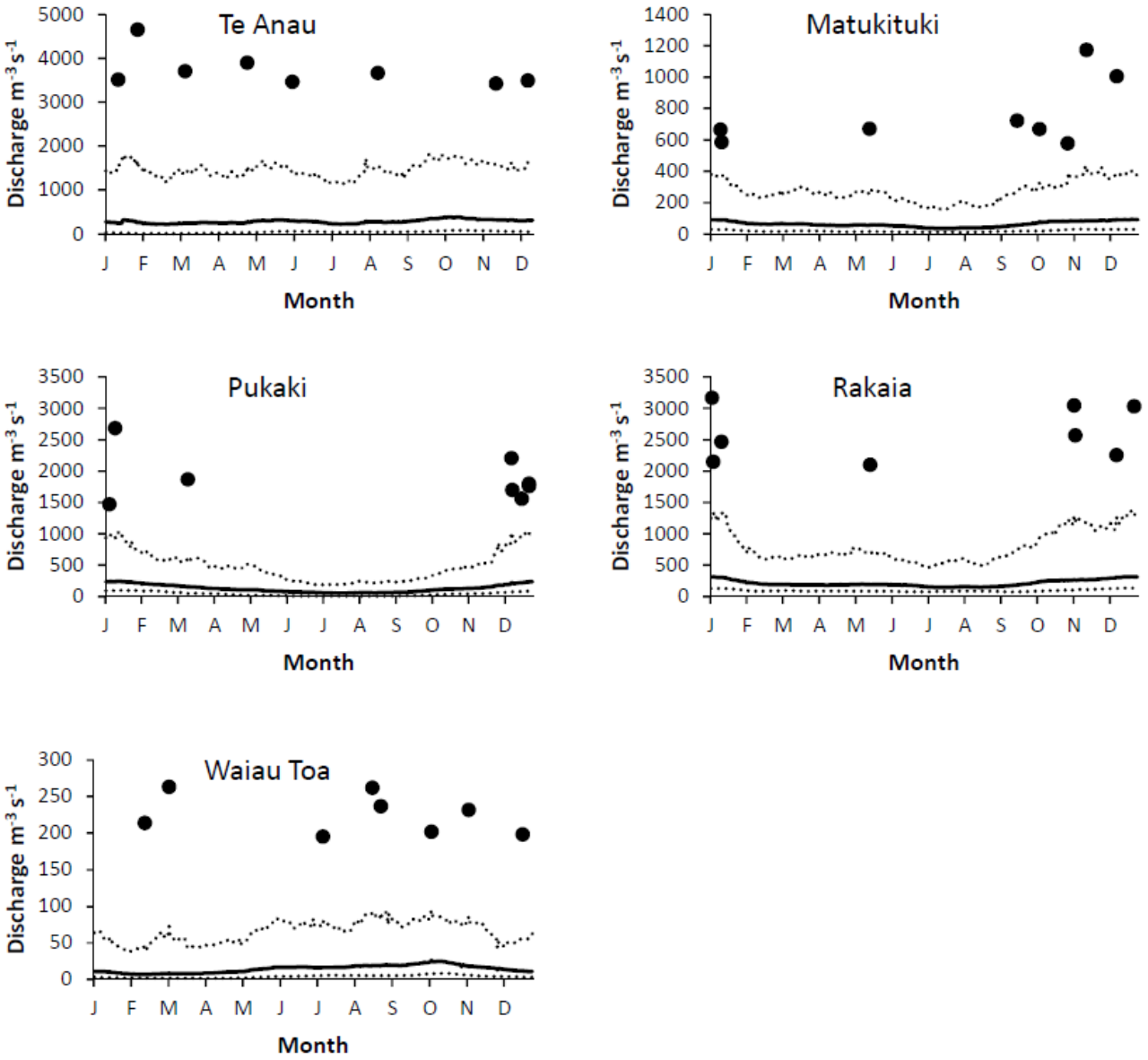

593

594 **Figure 2** Thirty-day running mean of mean (solid line), maximum and minimum (dotted lines) daily
595 river flow for 1979-2018 for the five study rivers, plus the top eight events for each catchment
596 (circles). Note the different y-axis scales.

597

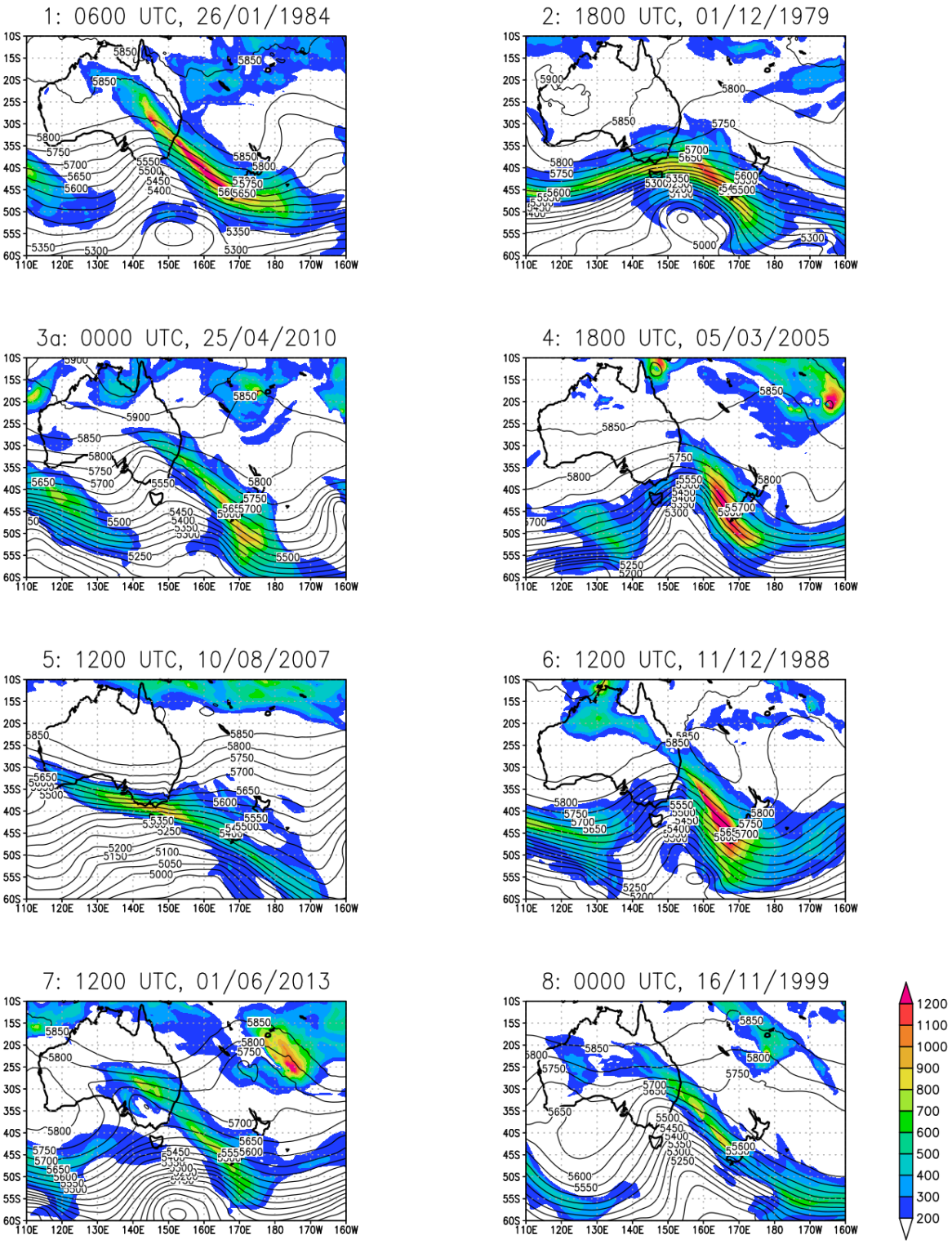

598

599 **Figure 3** IVT and 500 hPa geopotential height for the Te Anau top eight flow events.

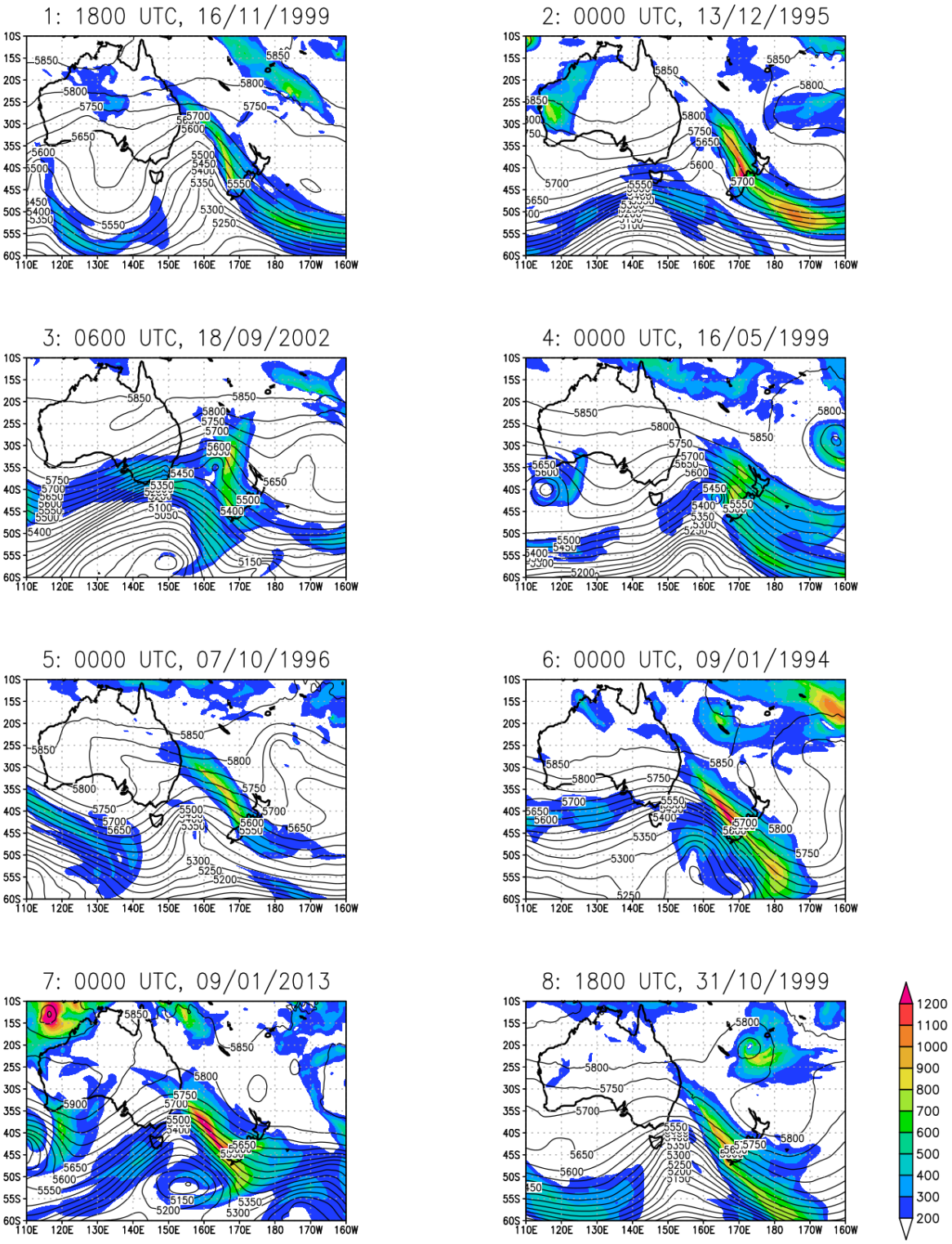

Figure 4 IVT and 500 hPa geopotential height for the Matukituki top eight flow events.

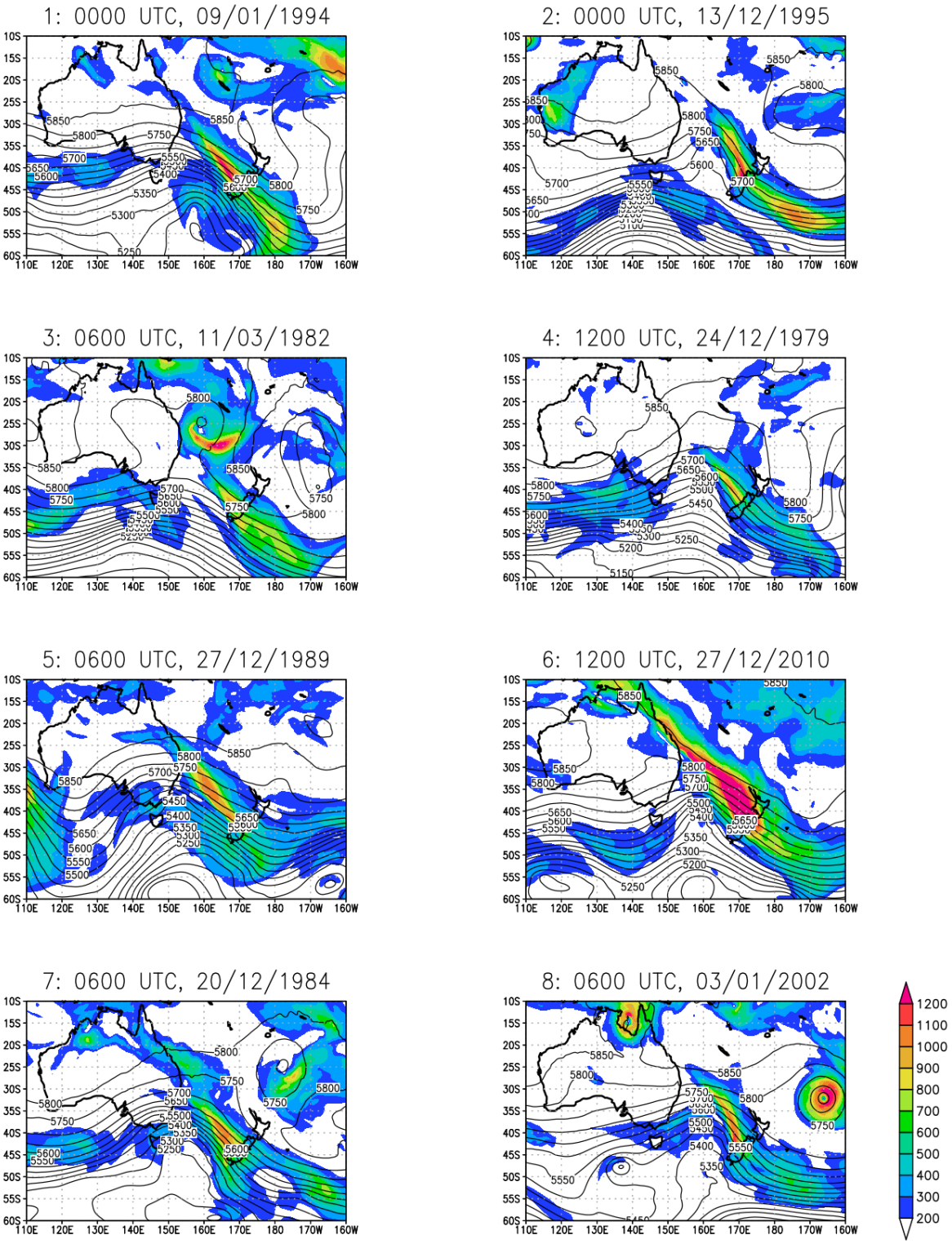

602

603 **Figure 5** IVT and 500 hPa geopotential height for the Pūkaki top eight flow events.

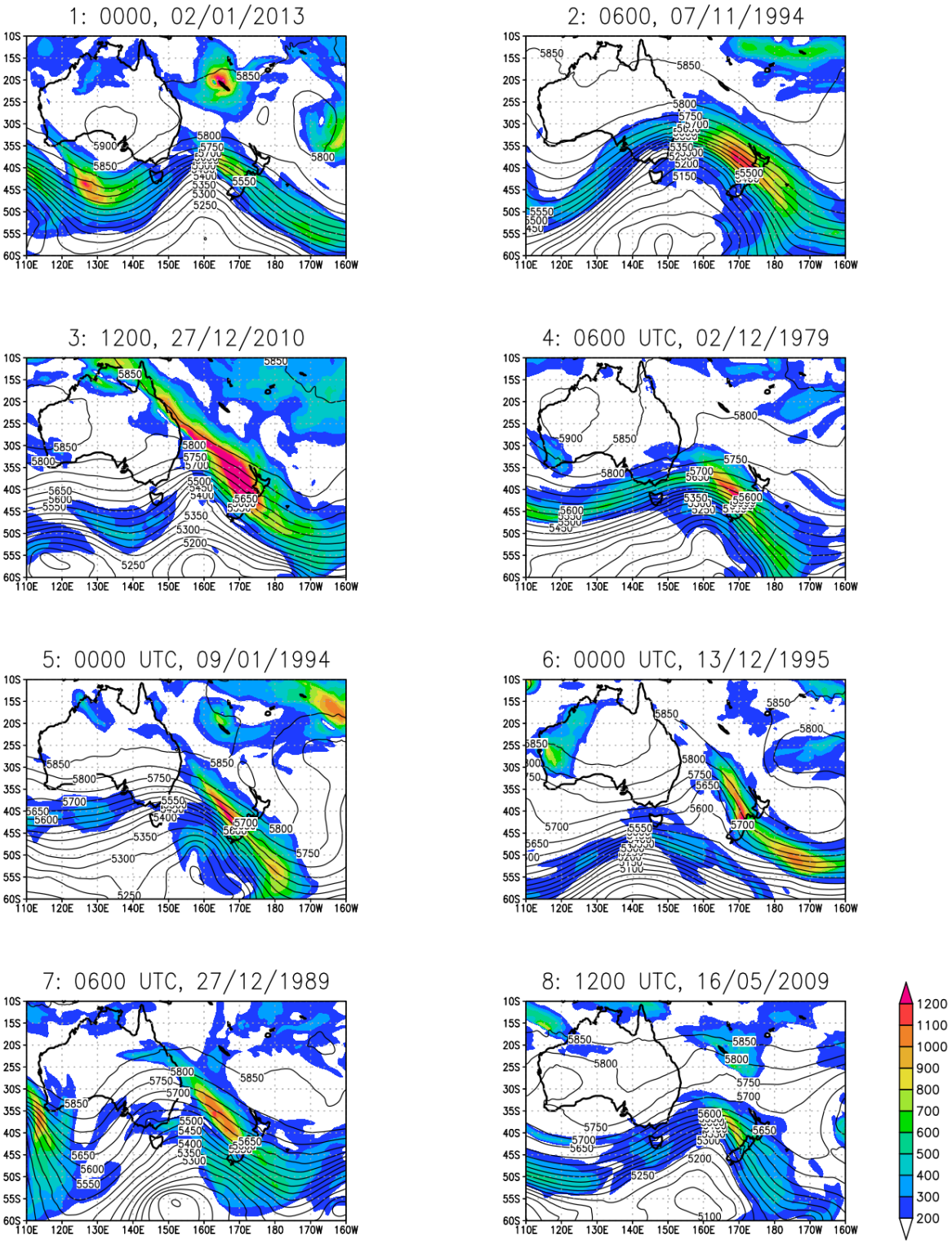

Figure 6 IVT and 500 hPa geopotential height for the Rakaia top eight flow events.

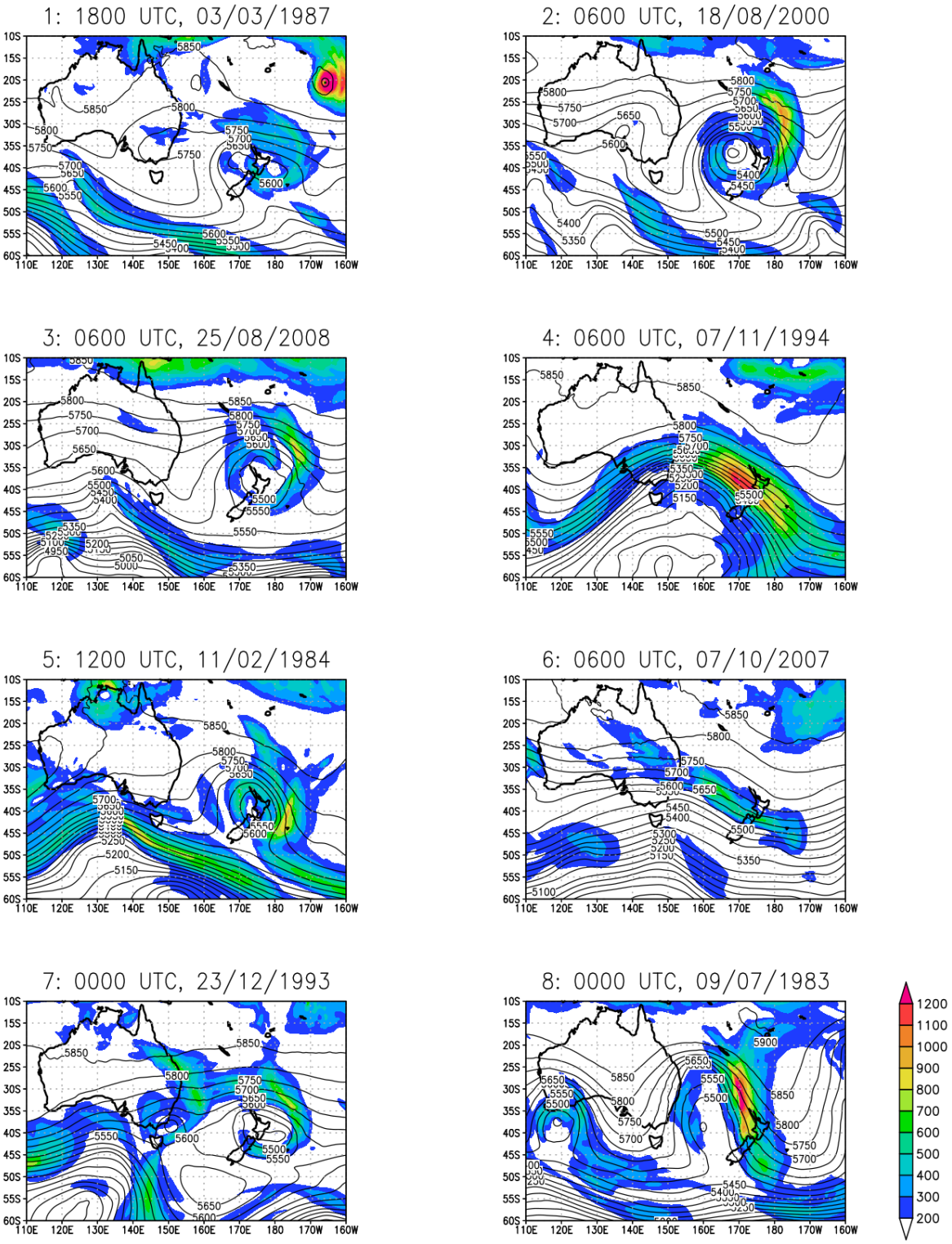

606

607 **Figure 7** IVT and 500 hPa geopotential height for the Waiau Toa top eight flow events.

608

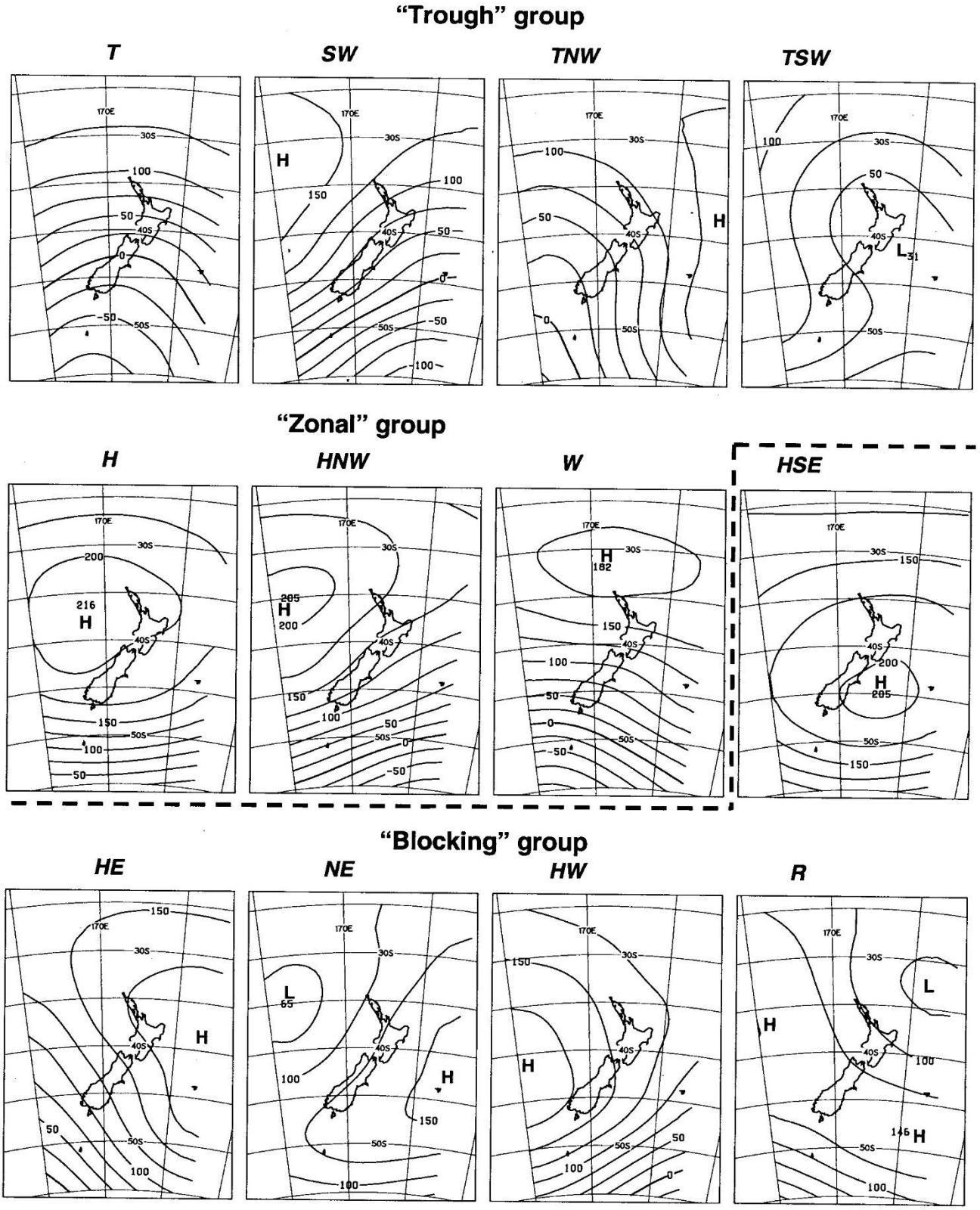

609

610 **Figure 8** 1000 hPa geopotential height composites for the 12 Kidson Weather Types (Kidson 2000).

611

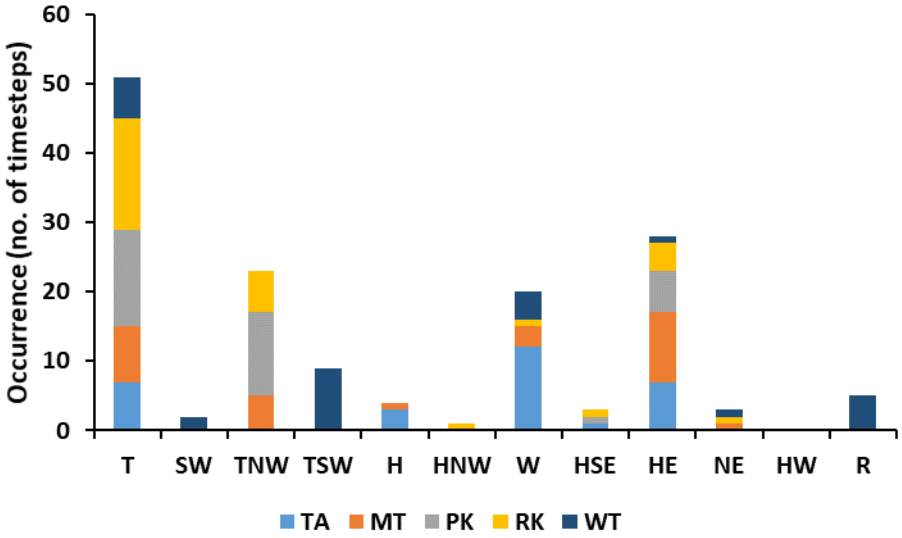

Figure 9 Occurrence (number of 12-hour timesteps) of different Kidson Weather Types during ascending limb of top eight flood events for each catchment (TA = Te Anau; MT = Matukituki; PK = Pūkaki; RK; RK = Rakaia; WT = Waiau Toa).

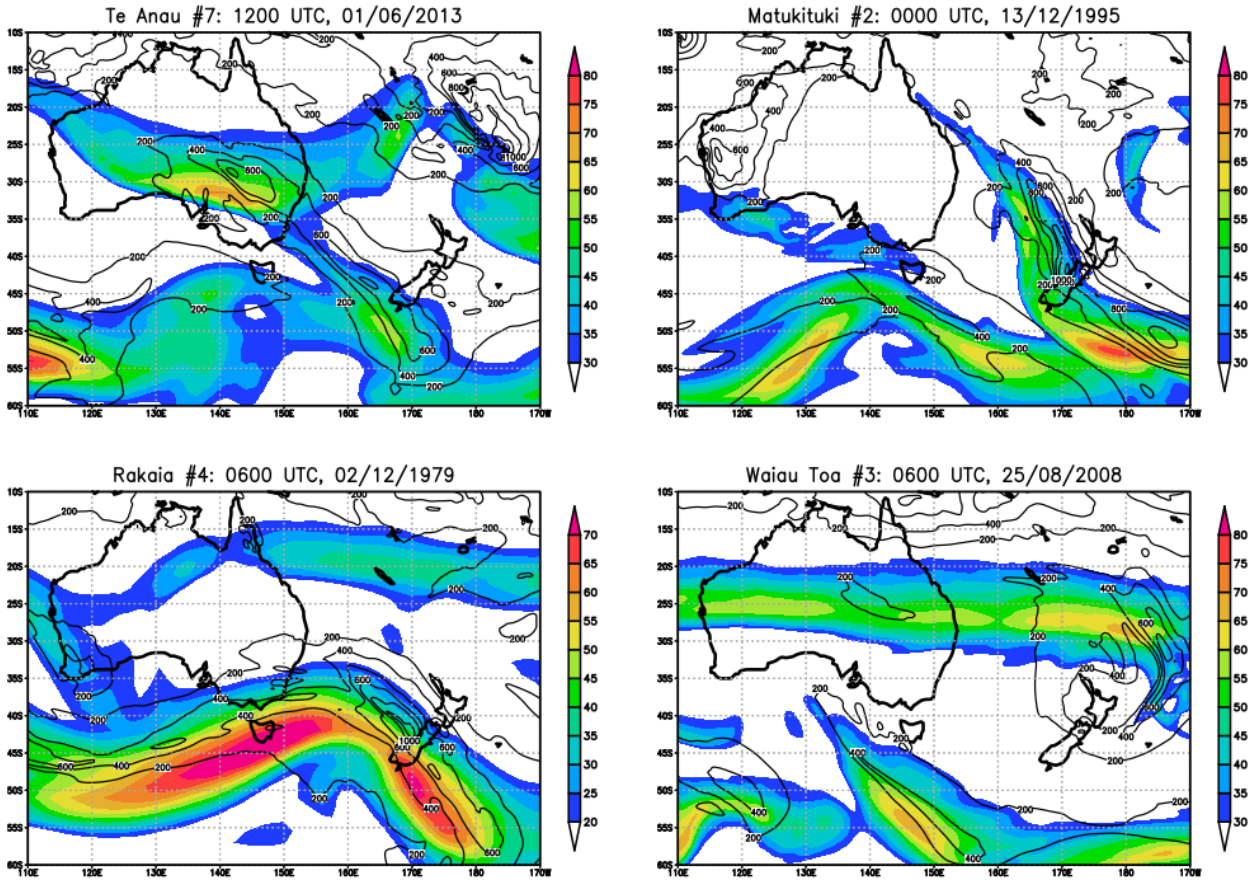

620

621 **Figure 10** 300 hPa wind speed (m s^{-1}, shading) and IVT (kg m^{-1} s^{-1}, isolines) for four exemplar high
622 flow events.